Geomechanics and Engineering, *Vol. 20, No. 4 (2020) 287-297*
DOI: https://doi.org/10.12989/gae.2020.20.4.287

Pseudo-static stability analysis of wedges based on the nonlinear Barton-Bandis failure criterion

Lianheng Zhao[1,2], Kangfu Jiao[1a], Shi Zuo*[1], Chenghao Yu[1] and Gaopeng Tang[1]

[1]*School of Civil Engineering, Central South University, Changsha, Hunan 410075, China*
[2]*Key Laboratory of Heavy-Haul Railway Engineering Structure, Ministry of Education, Central South University, Changsha, Hunan 410075, China*

(Received November 26, 2018, Revised January 27, 2020, Accepted January 28, 2020)

Abstract. This paper investigates the stability of a three-dimensional (3D) wedge under the pseudo-static action of an earthquake based on the nonlinear Barton-Bandis (B-B) failure criterion. The influences of the mechanical parameters of the discontinuity surface, the geometric parameters of the wedge and the pseudo-static parameters of the earthquake on the stability of the wedge are analyzed, as well as the sensitivity of these parameters. Moreover, a stereographic projection is used to evaluate the influence of pseudo-static direction on instability mode. The parametric analyses show that the stability coefficient and the instability mode of the wedge depend on the mechanical parameter of the rock mass, the geometric form of the wedge and the pseudo-static state of the earthquake. The friction angle of the rock φ_b, the roughness coefficient of the structure surface *JRC* and the two angles related to strikes of the joints θ_1 and θ_2 are sensitive to stability. Furthermore, the sensitivity of wedge height *h*, the compressive strength of the rock at the fracture surface *JCS* and the slope angle α to the stability are insignificant.

Keywords: three-dimensional rock wedge; pseudo-static stability analysis; nonlinear Barton-Bandis failure criterion; stereographic projection; design charts

1. Introduction

The stability of jointed rock slopes has always been an interesting and difficult topic within rock slope research. A great deal of research has been carried out in the past few decades on the stability of jointed rock slopes. Commonly used research methods include limit analysis (Chen *et al.* 2003, Florkiewicz and Kubzdela 2013), limit equilibrium (Fellenius 1936, Janbu 1954, Sarma 1979, Feng 1999) and numerical analysis (Zhou *et al.* 2015). Wang *et al.* (2015) proposed a limit analysis model for single-layer sliding surfaces to analyze any block model, based on the principles of limit analysis. Shukla (2011) derived a general analytical expression for the factor of safety of a multi-directional anchored rock slope (MDARS) against plane failure, incorporating most of the practically occurring destabilizing forces under surcharge and seismic loading conditions. However, the effects of dynamic load on the stability of two groups of joint wedge rock slopes has been seldom studied. Meanwhile, most scholars only consider the effect of the horizontal seismic activity and ignore the effect of the vertical seismic activity, although Zhao *et al.* (2017) showed that the influence of vertical seismic forces cannot be ignored—especially when the influence coefficient of horizontal earthquake is large.

This study shows that the shear properties of rough rock surface do not always satisfy the linear Mohr-Coulomb (M-C) criterion. Increasingly, nonlinear failure criteria are used to evaluate the stability of rock slopes (Barton and Choubey 1977, Bandis *et al.* 1981, Liu *et al.* 2010, Choi and Chung 1999, Jiang 2009, Zhao *et al.* 2015) among them, the Barton-Bandis (B-B) joint shear strength empirical criterion proposed by Barton is most commonly used. Li *et al.* (2009) and Feng and Lajtai (1998) analyzed the stability of slopes using the linear M-C criterion and the nonlinear B-B criterion. Luo *et al.* (2013) discussed the common methods of transforming the B-B failure criterion parameter into the linear M-C criterion shear strength parameter. Lin and Li (2014) developed a pseudo-static analysis method for the stability of anchored rock slope stability based on the JRC-JMC model. In their model considering of the influence of crack depth, seismic load, anchorage effect and structural plane parameters on the stability of a slope, a pseudo-static analysis method for the stability of anchored rock slope stability was established. Basha and Moghal (2013) and Nagpal and Basha (2012) combined the B-B criterion with reliability theory to analyze the influence of bolt and earthquake action on the stability of plane sliding rock slopes. Zhao *et al.* (2015) developed a method combining the B-B criterion with reliability theory to analyze the influence of hydraulics on the stability of plane sliding rock slopes with inclined fractures. However, the multiple failure modes that may exist during failure have rarely been taken into account in the above studies. Additionally, these studies are based on two-dimensional (2D) models, which is different from real three-dimensional (3D) force. The stability analysis of this slopes type involves resolution of

*Corresponding author, Ph.D.
E-mail: zuoshi@csu.edu.cn
[a]M.A.
E-mail: csu_jkf@csu.edu.cn

ISSN: 2005-307X (Print), 2092-6219 (Online)

forces in 3D space. The problem has received considerable attention in the literature (Londe 1969, Yang 2015). Also, the mechanisms leading to wedge failures in rock slopes have been extensively studied in the literature (Nathanail 1966). Johari and Lari (2016) and Li *et al.* (2009) analyzed the reliability of the 3D wedge with the influence of water pressure but assumed that the shear strength criterion of rock joints is subject to the linear M-C criterion.

Thus far, a variety of methods have been invented to analyze the behavior of slopes under seismic forces (Li *et al.* 2019), such as the pseudo-static method (Nouri *et al.* 2008, Zhao *et al.* 2016), the pseudo-dynamic method (Basha and Babu 2010, Qin and Chian 2018) and Newmark sliding-block analysis (Liang and Knappett 2017, Du 2018). The pseudo-static method was first employed by Terzaghi (1950) and was the most commonly used method for its simplicity and convenience. For slope stability analysis, limit equilibrium method (LEM) is widely used by engineers and researchers which is a traditional and well-established method. The pseudo-static approach has been implemented in various limit equilibrium methods to determine the safety factor (Loukidis *et al.* 2003). It manages to provide a fair estimation of the safety factor, with minimal computational cost compared with other methods. And for this reason, the method is favored by engineers.

Based on the above considerations, in this paper, the safety factor expression of a rock wedge slope is deduced based on the seismic pseudo-static method, and both the horizontal and vertical seismic effects are considered. To verify the accuracy and applicability of this method, theoretical calculations are compared with the discrete element numerical simulation results. The influence of the seismic pseudo-static direction on the instability mode is analyzed using the stereographic projection method. The influence of geometrical parameters, rock mechanics parameters, seismic pseudo-static parameters, and rock mechanics parameters on the safety factor of wedges are also analyzed.

2. Failure model based on nonlinear Barton-Bandis criterion

2.1 Nonlinear Barton-Bandis criterion

Barton and Choubey (1977) and Bandis *et al.* (1981) summarized the shear strength behavior of artificially produced rough, clean "joints.", and proposed the Barton-Bandis model. The nonlinear empirical formula of the *JRC-JCS* model for calculating the shear strength of joints is summarized as follows:

$$\tau = \sigma_n \tan[\varphi_b + JRC\log_{10}(JCS/\sigma_n)] \quad (1)$$

where τ is the shear strength of a rough rock surface, σ_n is the compressive strength of the rock on the discontinuity surface, *JRC* is the joint roughness coefficient, *JCS* is the compressive strength of the rock at the fracture surface and φ_b is the friction angle of the rock. In practical applications, the values of parameters *JRC*, *JCS* and φ_b can be referenced in the literature (Barton and Choubey 1977, Liu *et al.* 2005, Xia and Sun 2002). The literature notes that Eq. (1) is proposed under low-stress conditions. Therefore, the suitable range for Eq. (1) is $0.01 < \sigma/\sigma_c < 0.3$ (where σ_c is the uniaxial compressive strength of the rock). In Eq. (1), $[\varphi_b + JRC\log_{10}(JCS/\sigma_n)]$ should be no greater than 70°. In practical applications, the *JRC*, *JCS*, and φ_b values can be estimated based on experience or existing standards (He *et al.* 2012).

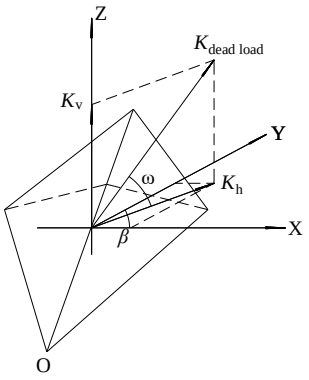

Fig. 1 Force diagram of a 3D wedge

2.2 Seismic pseudo-static analysis

In a 2D plane analysis, the pseudo-static method is often used for the dynamic stability analysis of the geotechnical structure (Baker and Garber 2016) to consider the complexity of the seismic action. For the seismic force, the horizontal seismic influence coefficient is K_h and the vertical seismic influence coefficient is K_v, which can usually be related according to:

$$K_v = \xi K_h \quad (2)$$

where ζ is the proportional coefficient of the vertical earthquake; if ζ is positive, the direction of force is the same as the positive direction of the Z axis and if ζ is negative, the direction of force is the same as the negative direction of the Z axis. The above method is used in this paper for the stability analysis of the 3D wedge. The force diagram of a wedge is shown in Fig. 1.

The effect of seismic pseudo-static force is calculated according to Eq. (3).

$$\begin{cases} K_v = \xi K_h \\ K_{hy} = K_h \sin(\beta) \\ K_{hx} = K_h \cos(\beta) \end{cases} \quad (3)$$

A clear model for analysis has been established to analyze the stability of sliding rock slopes. The pseudo-static force is applied to the three axes of the analytical model to consider the effect of seismic activity on the stability of the slope. Then, the pseudo-static earthquake and the gravity of the rock block are superimposed. The forces acting on the three coordinate axes, X, Y and Z, are expressed as t_1, t_2 and t_3, respectively. The space force vector form (t_1, t_2, t_3) could be calculated as follows:

$$\begin{cases} t_1 = K_h \cos(\beta) W \\ t_2 = K_h \sin(\beta) W \\ t_3 = (K_v - 1)\cos(\beta) W \end{cases} \quad (4)$$

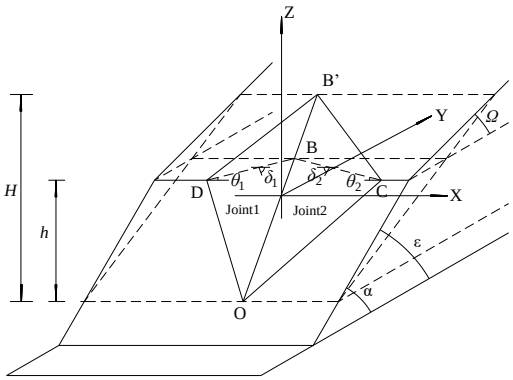

Fig. 2 Stability analysis model of a 3D wedge

2.3 Analytical model

Wittke (2015), Goodman (1989) and Low (1997) discussed the possible failure modes of a 3D wedge. Li *et al.* (2009) and Johari *et al.* (2016) analyzed four possible failure modes of wedges with fissure water pressure. There are also four possible modes of failure in the wedges under seismic pseudo static force: 1) sliding along discontinuity plane 1 only; 2) sliding along discontinuity plane 2 only; 3) sliding along the line of intersection of two discontinuity planes forming the block; 4) the wedge is separated from the two structural faces and is separated from the slope. It is assumed that all forces act through the center of gravity of the wedge so no moments are generated, and there is no rotational slip or toppling.

In this paper, the analysis model shown in Fig. 2 is selected to conduct research. In the Fig. 2, H is the height of the slope; h is the height of the wedge; α, Ω and ε are the inclination angles of the slope face, upper slope surface, and intersection of the two discontinuity planes, respectively; δ_1 and δ_2 denote the dips of the discontinuity planes 1 and 2, respectively; and θ_1 and θ_2 are the two angles in the horizontal triangular BDC, which are related to the strikes of the joints.

2.4 Wedge failure mechanism

Based on the analytical model, the safety factor of rock slopes is solved by considering the static equilibrium condition between the anti-slip effect and the sliding effect. The expression is shown as follows (Hoek and Bray 1981, Sharma *et al.* 1995, Wyllie *et al.* 2004):

$$Fs=\frac{F_{\text{resist}}}{F_{\text{induce}}} \tag{5}$$

where F_{resist} is the total anti-slip force and the F_{induce} is the sliding force.

In this paper, the closed-form equations for determining the safety factor of failure modes proposed by Low (1997) is referenced, and the expression of safety factor based on the B-B criterion can be obtained.

Failure Mode 1: sliding along plane 1 only

When Eq. (7) is satisfied, the wedge will slip along plane 1 only and the safety factor can be calculated by Eq. (6).

$$Fs_1=\frac{\left(\frac{\eta_1}{\eta_2}+\frac{\eta_2}{\eta_3}Z\right)\tan\left[\varphi_1+JRC_1\log_{10}\left(\frac{JCS_1\times s_1}{\eta_1+\eta_2\times Z}\right)\right]}{\sqrt{1+\left(\frac{\eta_2}{\eta_3}\sin\psi\right)^2}} \tag{6}$$

$$\begin{cases}\eta_2<0\\ \eta_1+\eta_2\times Z<0\end{cases} \tag{7}$$

The parameters η_1, η_2, η_3, s_1, and s_2 depend on the geometry of the wedge and the seismic pseudo-static parameters and can be calculated by:

$$\eta_3=\begin{bmatrix}(\sin\delta_2\cos\delta_1\cos\theta_2-\sin\delta_1\cos\delta_2\cos\theta_1)t_1\\ -(\sin\delta_2\cos\delta_1\sin\theta_2+\sin\delta_1\cos\delta_2\sin\theta_1)t_2\\ -\sin\delta_1\sin\delta_2\sin(\theta_1+\theta_2)t_3\end{bmatrix}/\sin(\psi) \tag{8}$$

$$\eta_1=-\frac{\cos\theta_2\times(t_1-\frac{\eta_3\times a_1}{\sin(\psi)})-\sin\theta_2\times(t_2-\frac{\eta_3\times a_2}{\sin(\psi)})}{\sin\sigma_1\sin(\theta_1+\theta_2)} \tag{9}$$

$$\eta_2=-\frac{\cos\theta_1\times(t_1-\frac{\eta_3\times a_1}{\sin(\psi)})-\sin\theta_1\times(t_2-\frac{\eta_3\times a_2}{\sin(\psi)})}{\sin\sigma_2\sin(\theta_1+\theta_2)} \tag{10}$$

$$\begin{cases}s_1=S_{\Delta OBC}=\dfrac{h^2k}{2\sin\delta_2\tan\varepsilon\sin\theta_2}\\ s_2=S_{\Delta OBD}=\dfrac{h^2k}{2\sin\delta_1\tan\varepsilon\sin\theta_1}\end{cases} \tag{11}$$

with:

$$a_1=\sin\delta_2\cos\delta_1\cos\theta_2-\sin\delta_1\cos\theta_1\cos\delta_2 \tag{12}$$

$$a_2=-\sin\delta_2\cos\delta_1\sin\theta_2-\sin\delta_1\cos\delta_2\sin\theta_1 \tag{13}$$

$$a_3=-\sin\delta_1\sin\delta_2\sin\theta_1\cos\theta_1-\sin\delta_1\sin\delta_2\sin\theta_2\cos\theta_1 \tag{14}$$

$$\sin\psi=\left|\sqrt{\{1-[\sin\delta_1\sin\delta_2\cos(\theta_1+\theta_2)+\cos\delta_1\cos\delta_2]^2\}}\right| \tag{15}$$

$$\varepsilon=\arctan\left(\frac{\sin(\theta_1+\theta_2)}{\sin\theta_1\cot\delta_2+\sin\theta_2\cot\delta_1}\right) \tag{16}$$

$$\kappa=\frac{H}{h}=\frac{(1-\frac{\tan\Omega}{\tan\alpha})}{(1-\frac{\tan\Omega}{\tan\varepsilon})} \tag{17}$$

$$Z=\cos\delta_1\cos\delta_2+\sin\delta_1\sin\delta_2\cos(\theta_1+\theta_2) \tag{18}$$

Failure Mode 2: sliding along plane 2 only

If Eq. (19) is satisfied, the wedge will slip along plane 1 only and the safety factor can be calculated by Eq. (20).

$$\begin{cases}\eta_1<0\\ \eta_2+\eta_1\times Z>0\end{cases} \tag{19}$$

$$Fs_2=\frac{(\frac{\eta_2}{\eta_3}+\frac{\eta_1}{\eta_3}Z)\tan[\varphi_2+JRC_2\log_{10}(\frac{JCS_2\times s_2}{\eta_2+\eta_1\times Z})]}{\sqrt{1+\left(\frac{\eta_1}{\eta_3}\sin\psi\right)^2}} \tag{20}$$

Failure Mode 3: sliding along the line of intersection of

two discontinuity planes

The safety factor of this mode can be calculated by:

$$Fs_3=\frac{\eta_1}{\eta_3}\tan\left[\varphi_1+JRC_1\log_{10}\left(\frac{JCS_1\times s_1}{\eta_1}\right)\right]+\frac{\eta_2}{\eta_3}\tan\left[\varphi_2+JRC_2\log_{10}\left(\frac{JCS_2\times s_2}{\eta_2}\right)\right] \quad (21)$$

Eq. (21) is valid, and the wedge will slide along two joints when the following conditions are met:

$$\begin{cases}\eta_1>0\\ \eta_2>0\end{cases} \quad (22)$$

Failure Mode 4: separated from the two structural faces

When Eq. (23) is satisfied, the wedge separated from the two structural faces:

$$\begin{cases}\eta_1+\eta_2\times Z<0\\ \eta_2+\eta_1\times Z<0\end{cases} \quad (23)$$

According to the above analysis, the stability of the wedge is mainly influenced by the basic geometric parameters of the wedge, the mechanical parameters of the rock and the parameters of the seismic pseudo-static force. The influence of parameters on the stability of the wedge is studied for specific cases in the following section. The Selected values, in this paper for analysis are arbitrarily selected within the range of parameter values.

3. Examples and verification

3.1 Wedge stability analysis and comparison

In this paper, a stability analysis method for a 3D wedge under seismic pseudo-static action is proposed based on the nonlinear B-B failure criterion. The theoretical derivation is compared with the analytical results of the discrete element numerical simulation software 3DEC (Itasca Consulting Group, Inc, 2007a, 2007b) to verify the correctness of this method. The analysis model established by 3DEC is shown in Fig. 4. The parameters required for numerical simulation are obtained using the B-B criterion and the M-C criterion parameter transformation method, which was proposed by Hoek and Bray (1981) and verified by (Zhao 1998, Prassetyo 2017). Eqs. (24-26) are used to calculate the required parameters. The results of this example parameter conversion are listed in the appendix (Tables 3-6).

$$\varphi_i=\arctan\left(\frac{\partial\tau}{\partial\sigma_n}\right) \quad (24)$$

$$\frac{\partial\tau}{\partial\sigma_n}=\frac{\tan\left(JRC\log_{10}\frac{JCS}{\sigma_n}+\varphi_b\right)}{-\frac{\pi JCS}{180\ln 10}\left[\tan^2\left(JRC\log_{10}\frac{JCS}{\sigma_n}+\varphi_b\right)+1\right]} \quad (25)$$

$$\varphi_i=\arctan\left(\frac{\partial\tau}{\partial\sigma_n}\right) \quad (26)$$

To verify the accuracy of the proposed method in this paper, $K_h=0.1$, $\beta=90°$ and $\zeta=$ -1.0-1.0 were selected; rock geometric parameter values are shown in Table 1 and 2. Calculation results and relative errors of the two methods are shown in Fig. 4.

Table 1 Wedge geometry parameters

Parameter	δ_1(°)	δ_2(°)	θ_1(°)	θ_2(°)	h(m)	α(°)	$\Omega(m)$
Value	50	48	62	40	10-30	60	20

Table 2 Rock physical and mechanical parameters

Parameter	JCS_1(Mpa)	JCS_2(Mpa)	JRC_1	JRC_2	φ_{b1}(°)	φ_{b2}(°)
Value	10	10	9	9	32	32

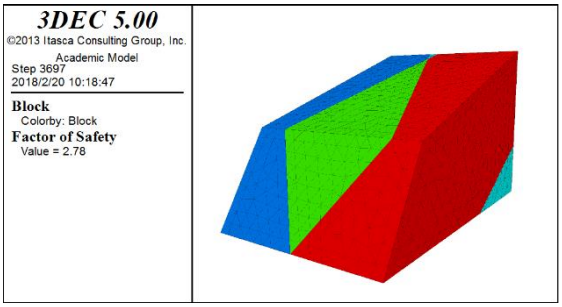

Fig. 3 Model diagram of 3DEC

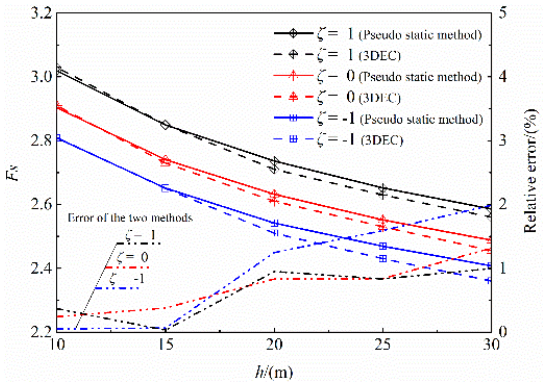

Fig. 4 Comparison of theoretical calculations and numerical simulation results

Fig. 4 shows that the relative error between theoretical calculation and numerical simulation results ranges from 0-3%. Therefore, the theoretical analysis of this paper is effective, considering the difference between theoretical calculations and the numerical simulation.

3.2 Wedge failure mode analysis and comparison

To further validate the methods in this article, the influence of seismic pseudo-static direction on the failure mode is analyzed. The parameters are set as follows: h = 10 m, $\delta_1=30°$, $\delta_2=40°$, $\theta_1=60°$, $\theta_2=50°$, $K_h=0.3$, $\zeta=1$. The theoretical calculation results of this paper are compared with the results of the stereographic projection. The results are shown in Figs. 5 and 6.

Fig. 5(a) shows the stereographic projection of the wedge model under the parameters of this example, where ○WSEN is the projected great circle, and plane 1 and plane 2 are the stereographic projections of joint 1 and 2, respectively. IO is the stereographic projection of the intersection of the two joints, OR is the stereographic projection of the resultant force of the wedge, and the arc

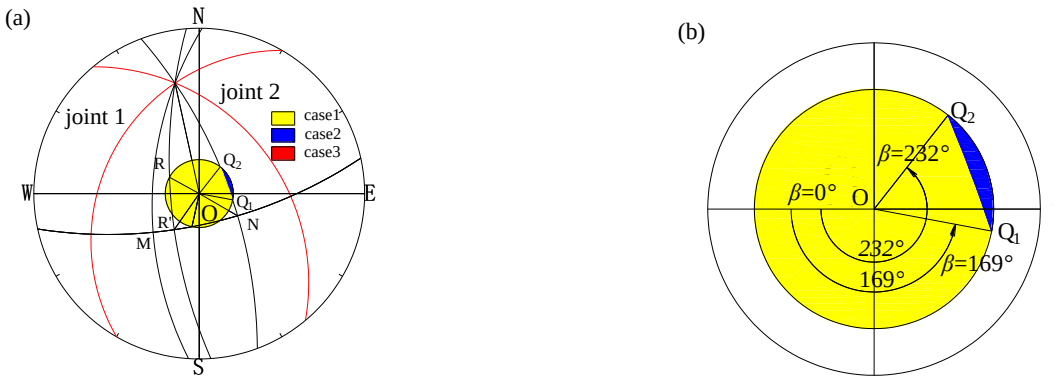

Fig. 5 The projection of the wedge

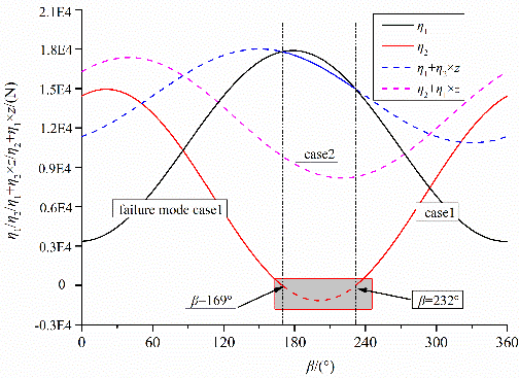

Fig. 6 Model diagram of 3DEC

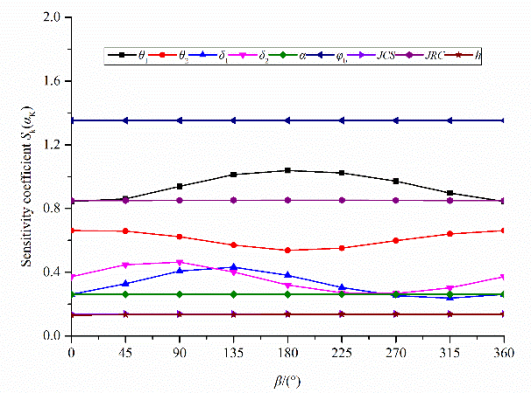

Fig. 7 Comparison of safety factor sensitivity coefficients for random variables

MN corresponds to the common vertical surface of the two joints. OM and ON represent the stereographic projection of the normal line of joint 1 and 2, respectively. OR' is a component of OR on the common vertical surface of the two joints.

Fig. 5(b) shows that failure mode 2 would occur when the value of β is within the interval (169°, 232°). Failure mode 1 occurs when β takes other values. The value of the discriminant of failure mode formulas (Eqs. (17, 18, 21, 23)) are calculated with a change of β.

It can be seen from Fig. 6 that a change of β can lead to a change in failure mode. The results of the method presented in this paper are consistent with the analytical results of the stereographic projection. This also indicates that the proposed method in this paper is correct and effective.

4. Parameter analysis

4.1 Parameter sensitivity analysis

Fig. 5(a) shows the stereographic projection of the wedge model under the parameters of this example, where ○WSEN is the projected great circle, and plane 1 and plane 2 are the stereographic projections of joint 1 and 2, respectively. IO is the stereographic projection of the intersection of the two joints, OR is the stereographic projection of the resultant force of the wedge, and the arc MN corresponds to the common vertical surface of the two joints. OM and ON represent the stereographic projection of the normal line of joint 1 and 2, respectively. OR' is a component of OR on the common vertical surface of the two joints.

$$S_K(\alpha_K)=(|\Delta P|/P)/(|\Delta\alpha_K|/\alpha_K);(K=1,2,3\cdots\cdots,n) \quad (27)$$

The corresponding sensitivity factor, $S_K^*(\alpha_K)$, is obtained by taking $\alpha_K = \alpha_K^*$.

Safety factor sensitivity coefficients for various pseudo-static directions are shown in Fig. 7. The parameters analyzed can be divided into two categories: rock mechanics parameters and wedge geometry parameters. It can be seen that φ_b is the most sensitive parameter regardless of changes in pseudo-static direction, followed by θ_1 and *JRC*.

4.2 Influence of seismic pseudo-static force on the stability of a wedge

The stability of a wedge is affected by the magnitude and direction of the seismic pseudo-static force. To explore the variation of the safety factor with the magnitude and direction of the seismic pseudo-static force, a graph was plotted in polar coordinates, as shown in Fig. 8. The parameters in Tables 1 and 2 were selected for analysis.

The distance from any point on the graph to the center of the circle represents the magnitude of the safety factor; arbitrary point angle coordinates represent the direction of

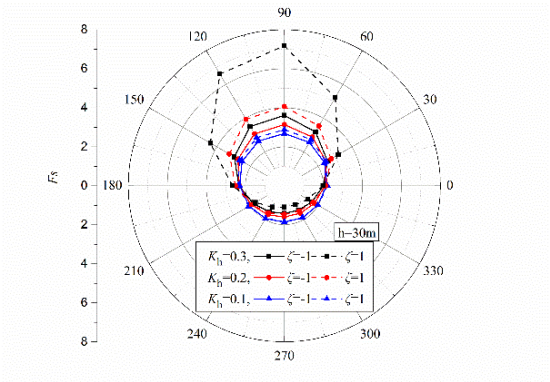

(a) The effect of ξ and β on the factor of safety

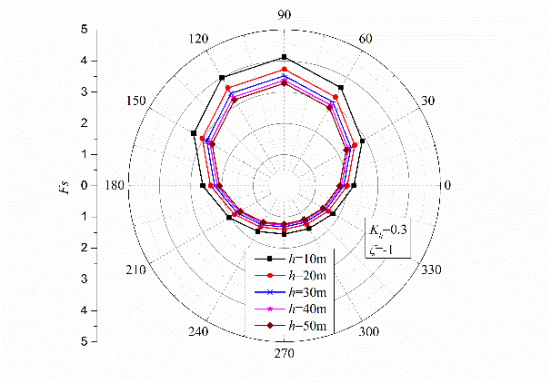

(b) The effect of h and β on the factor of safety

Fig. 8 Influence of seismic pseudo-static force on safety factor

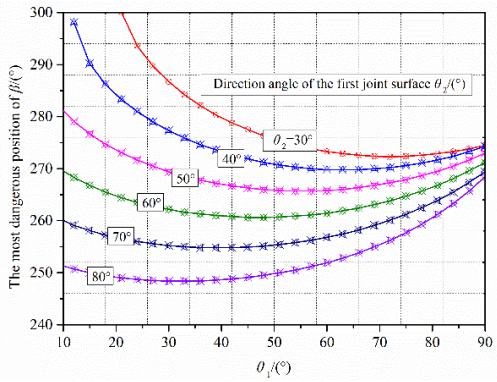

Fig. 9 Direction of the most dangerous seismic pseudo static forces for different geometrical forms of the wedge

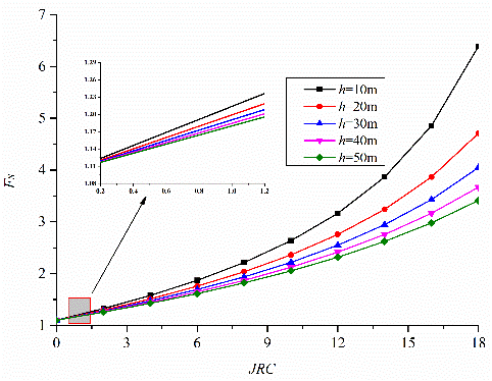

(a) The effect of *JRC* on the factor of safety

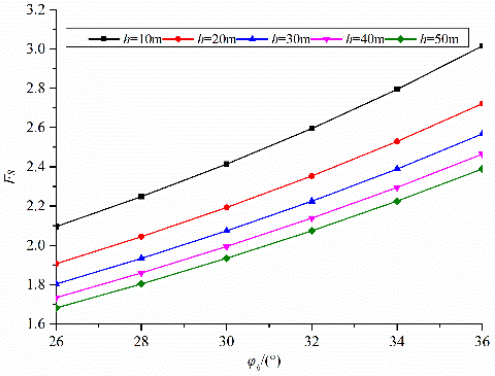

(b) The effect of φ_b on the factor of safety

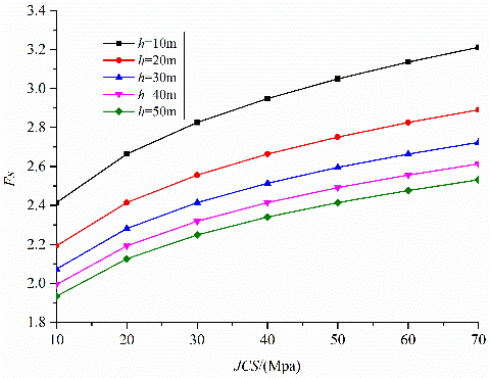

(c) The effect of *JCS* on the factor of safety

Fig. 10 Influence of rock mechanics parameters on safety factor

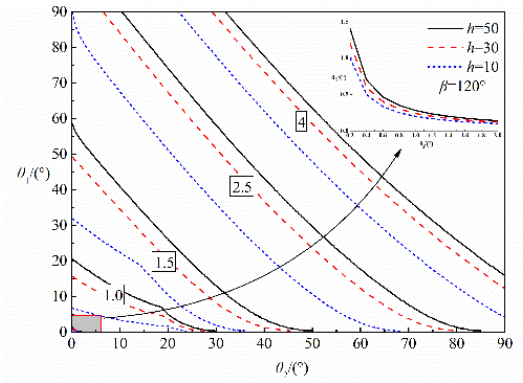

(a) β=120°

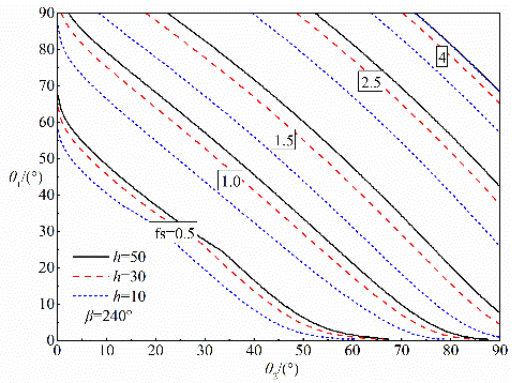

(b) β=240°

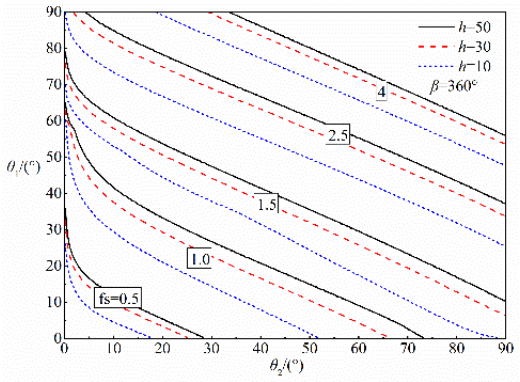

(c) β=360°

Fig. 11 Influence of rock mechanics parameters on safety factor

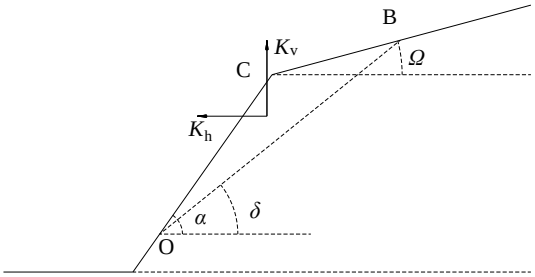

Fig. 12 The 2D analysis model

the seismic pseudo-static force.

Based on the above analysis, the safety factor changes greatly with the seismic pseudo-static direction. When the seismic pseudo-static direction is similar to the slope inclination, the wedge is in a more dangerous state and the safety factor is smaller. When the seismic pseudo-static direction and slope inclination are opposite, the wedge is in a stable state and the safety factor is larger. Fig. 9 shows the direction of the most dangerous seismic pseudo-static forces for different geometrical forms of the wedge.

Fig. 9 shows us that (1) when θ_2 is fixed, with increasing θ_1, the direction of the most dangerous seismic pseudo-static forces decreases, then increases; (2) when θ_1 is fixed, with increasing θ_2, the direction of the most dangerous seismic pseudo-static forces decreases as it approaches the negative X-axis.

4.3 Influence of rock mechanics parameters on the stability of the wedge

To analyze the influence of rock mechanics parameters on wedge stability, the parameters listed in Tables 1 and 2 were used for analysis. The results are shown in Fig. 10.

Fig. 10 shows that with increasing *JRC*, φ_b and *JCS* wedge stability increase. Hence, the influence of seismic pseudo-static force on the stability of a rock mass should be analyzed based on the actual mechanical parameters of the rock mass.

4.4 Influence of the combination of seismic pseudo-static force and wedge geometry on the stability of the wedge

To analyze the combined influence of wedge geometry and seismic pseudo-static form on the wedge safety factor, the parameters were set as follows to determine the safety factor: γ = 27 kN/m3, Ω = 0°, α = 60°, *JRC* = 9, *JCS* = 10 MPa, K_h = 0.2, ζ = 1. The results are presented in Fig. 11.

The influences of geometrical changes on the wedge safety factor are shown in Fig. 11. θ_1 and θ_2 are the angles related to the strikes of the joints. Note that a change in the combination of wedge shape and pseudo-static force can lead to a large change in the safety factor. For instance, when $\theta_1 = \theta_2 = 20°$ and β = 120°, the safety factor is greater than 1.5 (Fig. 11(a)), but when $\theta_1 = \theta_2 = 20°$ and β = 240°, the safety factor is reduced to less than 0.5 (Fig. 11(b)). When β changes from 120° to 240°, the force changes from pointing to the inside of the slope to the outside of the slope, which is not conducive to the stability of the wedge. Additionally, the safety factor increases with increased θ_1 and θ_2.

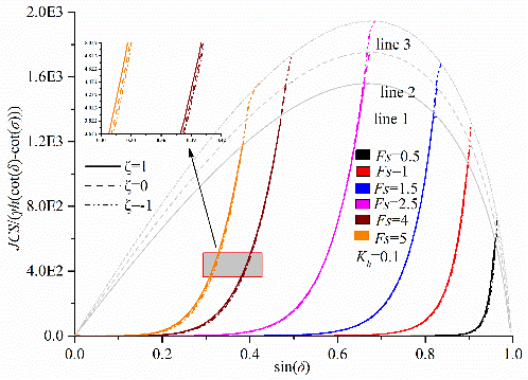

(a) K_h=0.1

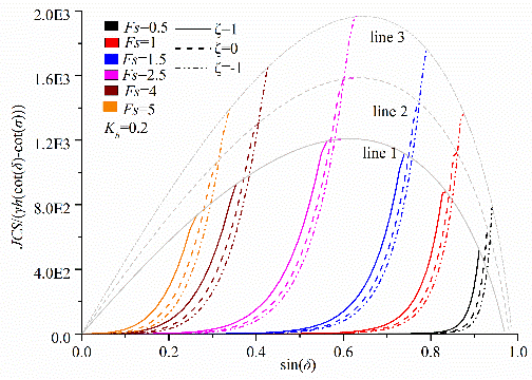

(b) K_h=0.2

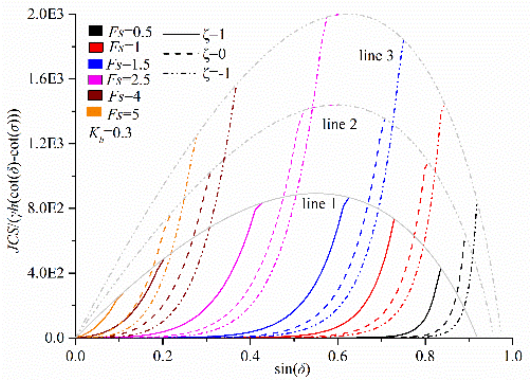

(c) K_h=0.3

Fig. 13 Influence of rock mechanics parameters on safety factor

4.5 Additional explanations for 2D situations

The 3D wedge model described above is not valid when the parameters are certain values, such as $\theta_1 = 0°$ or $\theta_2 = 0°$. Then, the research problem becomes that of an infinite body, and the formula obtained for the 3D-wedge model above can no longer be used. Next, a 2D calculation model is constructed that considers the above problems as shown in Fig. 12. The safety factor is plotted as shown in Fig. 13 with other parameters when $JRC = 9$ and $\varphi_b = 35°$.

In Fig. 13, using the dimensionless quantity $JCS/(\gamma h(\cot(\delta)\text{-}\cot(\alpha)))$ constituted by rock mechanics and geometric parameters and the sine value of the joint surface angle as vertical axis and horizontal axis, respectively, the change of the safety factor with the dimensionless quantity $JCS/(\gamma h(\cot(\delta)\text{-}\cot(\alpha)))$ and the sine value of the joint surface angle are studied. Fig. 13 shows that the stability of the rock slope decreases with increasing the joint surface angle and $JCS/(\gamma h(\cot(\delta)\text{-}\cot(\alpha)))$, but it will not increase without limit because the B-B failure criterion limits $[\varphi_b + JRC\log10\ (JCS/\sigma_n)]$ to 70°. This restriction results in an envelope. The envelope lines generated under different values in this paper are line1, line2 and line3. For points outside the envelope range, the safety factor values are the same as the points on the envelope with the same x-coordinate.

5. Conclusions

The friction angle of the rock φ_b, the roughness coefficient of the joint JRC and the two angles related to the directional of the space joint face θ_1 and θ_2 have larger sensitivity coefficients for various pseudo-static directions. Furthermore, the sensitivity of wedge height h, the compressive strength of the rock at the fracture surface JCS and the slope angle α to the stability are insignificant.

The change of the static force direction will change the failure mode of the wedge. It is known that failure mode 1 occurs in most cases. Failure modes 2 and 3 occur only when the seismic pseudo-static coefficient is large and the seismic pseudo-static direction is within a certain angle range.

The stability of the wedge is reduced by increasing the static coefficient. A change in the combination of wedge geometry and seismic pseudo-static force can lead to great fluctuations in the safety factor. In engineering, the magnitude of the earthquake force and the combination of seismic force and wedge geometry should be considered to ensure safety when conducting stability assessments.

Acknowledgments

This study was financially supported by the National Natural Science Foundation of China (Nos.51478477), Guizhou Provincial Department of Transportation Foundation (No. 2017122058 & No.2018123040), Guizhou Provincial Science and Technology Agency – Key Project of Technology Supporting Plan (No. [2018]2815). All financial supports are greatly appreciated.

References

Baker, R. and Garber, M. (1978), "Theoretical analysis of the stability of slopes", *Geotechnique*, **28**(4), 395-411. http://dx.doi.org/10.1680/geot.1978.28.4.395.

Bandis, S., Lumsden, A.C. and Barton, N.R. (1981), "Experimental studies of scale effects on the shear behaviour of rock joints", *Int. J. Rock Mech. Min. Sci.*, **18**(1), 1-21. http://dx.doi.org/10.1016/0148-9062(81)90262-X.

Barton, N. and Choubey, V. (1977), "The shear strength of rock joints in theory and practice", *Rock Mech.*, **10**(1), 1-54. http://dx.doi.org/10.1007/BF01261801.

Basha, B.M. and Babu, G.L.S. (2010), "Reliability assessment of internal stability of reinforced soil structures: A pseudo-dynamic approach", *Soil Dyn. Earthq. Eng.*, **30**, 336-353. http://dx.doi.org/10.1016/j.soildyn.2009.12.007.

Basha, B.M. and Moghal, A.A.B. (2013), "Load resistance factor design (LRFD) approach for reliability based seismic design of rock slopes against wedge failures", *Proceedings of the Geo-Congress 2013 on Design, Analysis and Performance of Rock Slopes and Rock Fill*, San Diego, California, U.S.A., March.

Chen, J., Yin, J.H. and Lee, C.F. (2003), "Upper bound limit analysis of slope stability using rigid finite elements and nonlinear programming", *Can. Geotech. J.*, **40**(4), 742-752. http://dx.doi.org/10.1139/t03-032.

Chen, W.F. (1975), *Limit Analysis and Soil Plasticity*, Elsevier Scientific Publishing Company, Amsterdam, The Netherlands.

Choi, S.O. and Chung, S.K. (2004), "Stability analysis of a jointed rock slope with the Barton-Bandis Joint Constitutive Model using UDEC", *Int. J. Rock Mech. Min. Sci.*, **41**(2), 581-586. http://dx.doi.org/10.1016/j.ijrmms.2004.03.103.

Du, W. (2018), "Effects of directionality and vertical component of ground motions on seismic slope displacements in Newmark sliding-block analysis", *Eng. Geol.*, **239**, 12-21. http://dx.doi.org/10.1016/j.enggeo.2018.03.012.

Feng, P. and Lajtai, E.Z. (1998), "Probabilistic treatment of the sliding wedge with EzSlide", *Eng. Geol.*, **50**(1), 153-163. http://dx.doi.org/10.1016/s0013-7952(98)00007-6.

Feng, S.R. (1999), "3D limit equilibrium method for slope stability and its application", *Chin. J. Geotech. Eng.*, **21**(6), 657-661.

Fellenius, W. (1936), "Calculation of the stability of earth dams", *Proceedings of the Transactions of the 2nd Congress on Large Dams*, Washington, D.C., U.S.A., *International Commission on Large Dams (ICOLD)*, Paris, France.

Florkiewicz, A. and Kubzdela, A. (2013), "Factor of safety in limit analysis of slopes", *Geomech. Eng.*, **5**(5), 485-497. https://doi.org/10.12989/gae.2013.5.5.485.

Goodman, R.E. (1989), *Introduction to Rock Mechanics*, John Wiley & Sons, New York, U.S.A.

He, J.M., Xu, M.H., Ma, D.X. and Cao, J. (2012), "The application of Barton structural plane shear strength formula in Murum Hydropower Station, Malaysia", *Resour. Environ. Eng.*, **5**, 542-544. http://dx.doi.org/10.16536/j.cnki.issn.1671-1211.2012.05.026.

Hoek, E. and Bray, J.W. (1981), *Rock Slope Engineering*, The Institution of Mining and Metallurgy, London, England, U.K.

Itasca Consulting Group, Inc. (2007a), *3DEC 4.1 Theory and Background*, Minneapolis, Minnesota, U.S.A.

Itasca Consulting Group, Inc. (2007b), *3DEC 4.1 Command Reference*, Minneapolis, Minnesota, U.S.A.

Itasca Consulting Group, Inc. (2017), Distinct element method, http://www.itascacg.com/software/products/udec/distinct-element-method.

Janbu, N. (1954), "Application of composite slip surfaces for stability analysis", *Proceedings of the European Conference on Stability of Earth Slopes*, Stockholm, Sweden, September.

Jiang, Q., Liu, X., Wei, W. and Zhou, C. (2013), "A new method for analyzing the stability of rock wedges", *Int. J. Rock Mech. Min. Sci.*, **60**(2), 413-422. http://dx.doi.org/10.1016/j.ijrmms.2013.01.008.

Jiang, Q.Q. (2009), "Stability of point safety factor of slope based on Hoek-Brown criterion", *J. Central South. Univ.*, **40**(3), 786-790. http://dx.doi.org/10.1016/S1874-8651(10)60073-7.

Jimenez-Rodriguez, R. and Sitar, N. (2007), "Rock wedge stability analysis using system reliability methods", *Rock Mech. Rock Eng.*, **40**, 419-427. http://dx.doi.org/10.1007/s00603-005-0088-x.

Johari, A. and Lari, A.M. (2016), "System reliability analysis of rock wedge stability considering correlated failure modes using sequential compounding method", *Int. J. Rock Mech. Min. Sci.*, **82**(3), 61-70. http://dx.doi.org/10.1016/j.ijrmms.2015.12.002.

Johari, A. and Lari, A.M. (2017), "System probabilistic model of rock slope stability considering correlated failure modes", *Comput. Geotech.*, **81**, 26-38. http://dx.doi.org/10.1016/j.compgeo.2016.07.010.

Li, C.C., Jiang, P.M and Zhou, A.Z. (2019), "Rigorous solution of slope stability under seismic action", *Comput. Geotech.*, **109,** 99-107. http://dx.doi.org/10.1016/j.compgeo.2019.01.018.

Liang, T. and Knappett, J.A. (2017), "Newmark sliding block model for predicting the seismic performance of vegetated slopes", *Soil Dyn. Earthq. Eng.*, **101**, 27-40. http://dx.doi.org/10.1016/j.soildyn.2017.07.010.

Li, D., Zhou, C., Lu, W. and Jiang, Q.H. (2009), "A system reliability approach for evaluating stability of rock wedges with correlated failure modes", *Comput. Geotech.*, **36**(8), 1298-1307. http://dx.doi.org/10.1016/j.compgeo.2009.05.013.

Lin, Y.L. and Li, X.X. (2014), "Pseudo-static analysis of seismic stabmty of anchored rock slope based on J_{RC}-J_{MC} failure criterion", *China Civ. Eng. J.*, **47**(S1), 269-273.

Liu, W.M., Fu, H. and Wu, J.L. (2005), "Current Situation of determination methods of shear strength parameters of rock-mass discontinuities and new thoughts", *J. ChongQing JiaoTong Univ.*, **24**(5), 65-67.

Liu, L.P., Yao, L.H., Chen, J. and Wang, C.H. (2010), "Rock slope stability analysis based on Hoke-Brown failure criterion", *Chin. J. Rock Mech. Eng.*, **29**(S1), 2879-2886. http://dx.doi.org/10.1016/j.compgeo.2016.07.010.

Londe, P., Vigier, G. and Vormeringer, R. (1969) "Stability of rock slopes, a three-dimensional study", *J. Soil Mech. Found. Div.*, **95**, 235-262.

Loukidis, D., Bandini, P. and Salgado, R. (2003), "Stability of seismically loaded slopes using limit analysis", *Geotechnique*, **53**, 463-479. http://dx.doi.org/10.1680/geot.2003.53.5.463.

Low, B.K. (1997), "Reliability analysis of rock wedges", *J. Geotech. Geoenviron. Eng.*, **123**(6), 498-505. http://dx.doi.org/10.1061/(ASCE)1090-0241(1997)123:6(498).

Luo, Q., Zhao, L.H., Li, L., Tan, H.H. and Luo, W. (2013), "Stability analysis of anchored rock slope based on Barton-Bandis failure criterion" *Rock Soil Mech.*, **34**(05), 1351-1359. http://dx.doi.org/10.16285/j.rsm.2013.05.004.

Nagpal, A. and Basha, B.M. (2012), "Reliability analysis of anchored rock slopes against planar failure", *Proceedings of the Indian Geotechnical Conference*, New Delhi, India.

Nathanail, C.P. (1996), "Kinematic analysis of active/passive wedge failure using stereographic projection", *Int. J. Rock Mech. Min. Sci. Geomech. Abstr.*, **33**(4), 405-407. http://dx.doi.org/10.1016/0148-9062(95)00079-8.

Nouri H., Fakher A. and Jones C.J.F.P. (2008), "Evaluating the effects of the magnitude and amplification of pseudo-static acceleration on reinforced soil slopes and walls using the limit equilibrium horizontal slices method", *Geotext. Geomembr.*, **26**, 263-278. http://dx.doi.org/10.1016/j.geotexmem.2007.09.002.

Prassetyo, S.H., Gutierrez, M. and Barton, N. (2017), "Nonlinear shear behavior of rock joints using a linearized implementation of the Barton-Bandis model", *J. Rock Mech. Geotech. Eng.*, **9**(4), 671-682. http://dx.doi.org/10.1016/j.jrmge.2017.01.006.

Qin, C.Q and Chian, S.C. (2018), "Seismic bearing capacity of non-uniform soil slopes using discretization-based kinematic analysis considering Rayleigh waves", *Soil Dyn. Earthq. Eng.*, **109**, 23–32 http://dx.doi.org/10.1016/j.soildyn.2018.02.017.

Sarma, S.K. (1979), "Stability analysis of embankments and slopes", *J. Geotech. Eng. Div.*, **105**(12), 1511-1524. http://dx.doi.org/10.1680/geot.1973.23.3.423.

Sharma, S., Raghuvanshi, T.K. and Anbalagan, R. (1995), "Plane failure analysis of rock slopes", *Geotech. Geol. Eng.*, **13**(2), 105-111. http://dx.doi.org/10.1007/BF00421876.

Shukla, S.K. and Hossain, M.M. (2011), "Stability analysis of multi-directional anchored rock slope subjected to surcharge and seismic loads", *Soil Dyn. Earthq. Eng.*, **31**(5-6), 841-844. http://dx.doi.org/10.1016/j.soildyn.2011.01.008.

Terzaghi K. (1950), *Mechanisms of Landslides, Engineering Geology (Berdey) Volume*, in *Geotechnical Society of America*, 83-125.

Xia, C.C. and Sun, Z.G. (2002), *Engineering Rock Mass Joint Mechanics*, Tongji University Press, Shanghai, China.

Wang, Z.D., Xia, Y.Y. and Xia, G.B. (2015), "Upper bound limit analysis method for stability analysis of bedding rock slopes", *Rock Soil Mech.*, **36**(2), 576-583. http://dx.doi.org/10.16285/j.rsm.2015.02.038.

Wittke, W. (2015), "Rock mechanics based on an anisotropic jointed rock model (AJRM)", *J. Rock Mech. Geotech. Eng.*, **7**(5), 607-608.

Wittke W. (2014), *Rock Mechanics Based on an Anisotropic Jointed Rock Model (AJRM)*, John Wiley & Sons.

Wyllie, D. (2004), *Rock Slope Engineering: Civil and Mining*, Spon Press, New York, U.S.A.

Yang, X.L. and Pan, Q.J. (2015), "Three dimensional seismic and static stability of rock slopes", *Geomech. Eng.*, **8**(1), 97-111. http://dx.doi.org/10.12989/gae.2015.8.1.097.

Zhang, G. and Zhu, W.S. (1993), "Parameter sensitivity analysis and test scheme optimization", *Rock Soil Mech.*, **14**(1), 51-58.

Zhao, J. (1998), "A new JRC-JMC shear strength criterion for rock joint", *Chin. J. Rock Mech. Eng.*, **17**, 349-357.

Zhao, L.H., Cao, J., Zhang, Y. and Luo, Q. (2015), "Effect of hydraulic distribution form on the stability of a plane slide rock slope under the nonlinear Barton-Bandis failure criterion", *Geomech. Eng.*, **8**(3), 391-414. http://doi.org/10.12989/gae.2015.8.3.391.

Zhao, L.H., Cheng, X., Zhang, Y., Li, L. and Li, D.J. (2016), "Stability analysis of seismic slopes with cracks", *Comput. Geotech.*, **77**, 77-90. http://dx.doi.org/10.1016/j.compgeo.2016.04.007.

Zhao, L.H., Cheng, X., Dan, H.C., Tang, Z.P. and Zhang, Y. (2017), "Effect of vertical earthquake component on the permanent seismic displacement of soil slopes based on the nonlinear Mohr-Coulomb failure criterion", *Soils Found.*, **57**(2), 237-251. http://dx.doi.org/10.1016/j.sandf.2016.12.002.

CC

Appendix

Table 3 The numerical value of c_1(MPA) calculated by B-B criterion and the M-C criterion parameter conversion formula under different conditions

h/ζ	-1	0	1
10	29.857	30.223	30.625
15	24.796	25.156	25.550
20	21.266	21.620	22.010
25	18.566	18.916	19.300
30	16.385	16.7311	17.111

Table 4 The numerical value of c_2(MPA) calculated by B-B criterion and the M-C criterion parameter conversion formula under different conditions

h/ζ	-1	0	1
10	0.029	0.027	0.025
15	0.045	0.042	0.039
20	0.062	0.057	0.053
25	0.079	0.073	0.067
30	0.096	0.089	0.082

Table 5 The numerical value of φ_1(°) calculated by B-B criterion and the M-C criterion parameter conversion formula under different conditions

h/ζ	-1	0	1
10	30.379	30.764	31.190
15	25.308	25.687	26.104
20	21.771	22.144	22.555
25	19.063	19.432	19.839
30	16.878	17.242	17.645

Table 6 The numerical value of φ_2(°) calculated by B-B criterion and the M-C criterion parameter conversion formula under different conditions

h/ζ	-1	0	1
10	29.857	30.223	30.625
15	24.796	25.156	25.550
20	21.266	21.620	22.010
25	18.566	18.916	19.300
30	16.385	16.7311	17.111